ARMY RESEARCH LABORATORY

New Outlook on the High-Pressure Behavior of Pentaerythritol Tetranitrate

by Jennifer A. Ciezak and Timothy A. Jenkins

ARL-TR-4238 **September 2007**

NOTICES

Disclaimers

The findings in this report are not to be construed as an official Department of the Army position unless so designated by other authorized documents.

Citation of manufacturer's or trade names does not constitute an official endorsement or approval of the use thereof.

Destroy this report when it is no longer needed. Do not return it to the originator.

Army Research Laboratory
Aberdeen Proving Ground, MD 21005-5066

ARL-TR-4238 **September 2007**

New Outlook on the High-Pressure Behavior of Pentaerythritol Tetranitrate

Jennifer A. Ciezak
Weapons and Materials Research Directorate, ARL

Timothy A. Jenkins
Geophysical Laboratory
Carnegie Institution of Washington

REPORT DOCUMENTATION PAGE	Form Approved OMB No. 0704-0188

1. REPORT DATE *(DD-MM-YYYY)*	2. REPORT TYPE	3. DATES COVERED (From - To)
September 2007	Final	October 2006–May 2007

4. TITLE AND SUBTITLE
New Outlook On the High-Pressure Behavior of Pentaerythritol Tetranitrate

5a. CONTRACT NUMBER

5b. GRANT NUMBER

5c. PROGRAM ELEMENT NUMBER

6. AUTHOR(S)
Jennifer A. Ciezak and Timothy A. Jenkins*

5d. PROJECT NUMBER

5e. TASK NUMBER

5f. WORK UNIT NUMBER

7. PERFORMING ORGANIZATION NAME(S) AND ADDRESS(ES)
U.S. Army Research Laboratory
ATTN: AMSRD-ARL-WM-BD
Aberdeen Proving Ground, MD 21005-5066

8. PERFORMING ORGANIZATION REPORT NUMBER
ARL-TR-4238

9. SPONSORING/MONITORING AGENCY NAME(S) AND ADDRESS(ES)
*Geophysical Laboratory, Carnegie Institution of Washington
5251 Broad Branch Rd. NW, Washington, DC 20015

10. SPONSOR/MONITOR'S ACRONYM(S)

11. SPONSOR/MONITOR'S REPORT NUMBER(S)

12. DISTRIBUTION/AVAILABILITY STATEMENT
Approved for public release; distribution is unlimited.

13. SUPPLEMENTARY NOTES

14. ABSTRACT

To gain insight into the high-pressure behavior of pentaerythritol tetranitrate ($C(CH_2ONO_2)_4$), single crystal Raman spectroscopy results were obtained for hydrostatic/quasi-hydrostatic and non-hydrostatic compression in a diamond anvil cell. Detailed analyses of the pressure-induced changes in the single-crystal/neon hydrostatic media revealed the splitting of several vibrational modes and many intensity fluctuations, which provide strong evidence for a pressure-induced symmetry modification from S_4 to D_2 rather than a high-pressure phase transition. Near 14.8 GPa, many vibrational features disappeared or significantly broadened. These spectral modifications were coincident with the appearance of cracks in the single crystal, which are believed to result from an elastic-plastic deformation attributable to slip plane activation. The effect of pressure media on the high-pressure behavior was also studied. The onset pressure of the S_4 to D_2 symmetry modification was found to be strongly dependent on the pressure media, but all single crystal samples that survived to 14.8 GPa were subject to the elastic-plastic deformation. If the pressure in the diamond anvil cell did not exceed 14.5 GPa, the samples could be quenched and recovered at ambient pressure; however, once the pressure exceeded 14.5 GPa and the slip planes became activated, the samples decomposed upon return to ambient conditions.

15. SUBJECT TERMS
PETN; vibrational spectroscopy; high-pressure; pentaerythritol tetranitrate; diamond anvil cell

16. SECURITY CLASSIFICATION OF:			17. LIMITATION OF ABSTRACT	18. NUMBER OF PAGES	19a. NAME OF RESPONSIBLE PERSON
a. REPORT	b. ABSTRACT	c. THIS PAGE			Jennifer A. Ciezak
UNCLASSIFIED	UNCLASSIFIED	UNCLASSIFIED	UL	26	19b. TELEPHONE NUMBER (*Include area code*) 410-306-1904

Standard Form 298 (Rev. 8/98)
Prescribed by ANSI Std. Z39.18

Contents

List of Figures

Acknowledgments

Dr. K. Clark of the Naval Surface Warfare Center, Indian Head, Maryland, is thanked for providing the pentaerythritol tetranitrate crystals. We also thank Dr. R.J. Hemley of the Geophysical Laboratory of the Carnegie Institute of Washington for valuable suggestions during the preparation of this manuscript.

INTENTIONALLY LEFT BLANK.

1. Introduction

A detailed understanding of the response of energetic materials to extreme conditions such as high temperature and pressure is crucial to addressing issues related to sensitivity, performance, and safety. Polymorphic phases of energetic materials commonly observed at elevated pressure or temperature have been shown to differ in their sensitivity and detonation parameters relative to the phase observed at ambient conditions (*1*). As a result of the different physical behaviors of the polymorphs, during extreme conditions, a deeper understanding of the molecular modifications associated with the polymorphic behavior of energetic materials is necessary for the proper characterization of the reactive behavior and may aid in the development of future munitions and methods for controlling sensitivity.

The static high-pressure behavior of the energetic material pentaerythritol tetranitrate (PETN) ($C(CH_2ONO_2)_4$), shown in figure 1, is a subject of continuing interest (*2–19*). Gruzdkov et al. first reported evidence for a phase transition in a single-crystal solid at pressures above 5 GPa (*14*). The static high-pressure experiments were performed in a diamond anvil cell in a glycerol pressure medium that maintained quasi-hydrostatic conditions to 9 GPa. A detailed comparison of the experimental vibrational frequencies obtained under these high-pressure conditions to the calculated frequencies of various conformers of PETN with different molecular symmetry provided evidence for a symmetry change (S_4 to C_2) under high-pressure (*14*). Subsequent experimental studies have reported modifications in the Raman spectral patterns, such as the appearance or disappearance of vibrational peaks, as well as large spectroscopic shifts of the Raman frequencies (*16*) to higher energies. These Raman experiments, in conjunction with x-ray diffraction results, which revealed splitting and shifting of several diffraction peaks (*19*), provide strong support for the existence of a high-pressure phase transition. In contrast to the Gruzdkov et al. study (*14*), these experiments used powdered PETN samples and different pressure media: neon gas as the pressure medium in the Raman

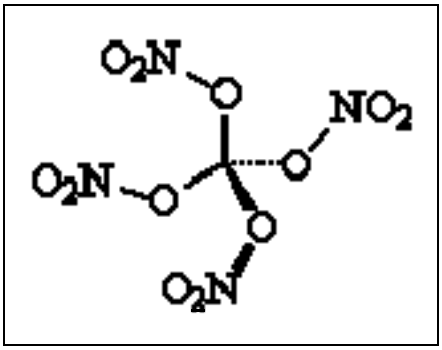

Figure 1. The molecular structure of pentaerythritol tetranitrate.

experiments and nitrogen for the x-ray diffraction experiment. Another recent Raman report, however, revealed no evidence of a phase transition to pressures near 31 GPa, even though the study was performed in the same conditions as the x-ray diffraction experiment (*15*).

In summary, although the static high-pressure behavior of PETN has received considerable attention in the past, the studies provide contradicting information about the existence of the high-pressure polymorph. It is evident that the pressurizing medium, which provides varying degrees of hydrostaticity, influences the high-pressure behavior, but these effects have not been fully investigated. In this work, we provide more detailed information about the response of PETN to static high pressure with the use of several pressure media, powder, and single-crystal samples. The primary goals of this work were to (1) examine changes in the internal vibrational modes of PETN as a function of pressure with the hydrostatic pressure medium neon, in an attempt to clarify the existence of the high-pressure phase transition, and (2) to investigate the effect of pressure media on pressure-induced changes in the crystal, including an examination of the effect of polycrystalline versus single-crystal samples on the high-pressure behavior.

2. Experimental Methodology

Polycrystalline PETN was obtained from the Naval Surface Warfare Center at Indian Head, Maryland. Single crystals of approximately 150–200 μm laterally with a thickness of 30–50 μm were selected from a polycrystalline sample and loaded into the center of the gasket hole. A small portion of the sample was carefully ground with a mortar and pestle into a fine powder with submicron particle sizes. For each experiment, a rhenium gasket pre-indented to a thickness of 60 μm was drilled with an electric discharge, creating a sample chamber of approximately 250 μm in diameter. For the experiments employing a pressure medium, the diamond anvil cell was loaded with nitrogen, neon, or helium gas according to previously published methods (*20*). The pressure on the sample was determined from the frequency shift of the ruby R_1 fluorescence line (*21*). The 488.0 laser line of an Argon ion laser (Coherent Innova 90) was used as the Raman excitation source, and the power output was limited to less than 0.5 W for the duration of the experiments. A 460-mm focal length *f*/5.3 imaging spectrograph (ISA HR 460) equipped with an 1800-groves/mm grating, which provides a spectral resolution of ±4.0 cm^{-1} was used for the Raman experiments. Before any experimental measurements, a wavelength calibration of the spectrograph was performed with a neon lamp; this method of calibration has an accuracy of ±1 cm^{-1} (*22*). For all experiments, an Olympus BX-40 microscope, with a spatial resolution of 5 μm was used to focus the laser onto the sample contained within the diamond anvil cell. All experiments were performed in the backscattering geometry at room temperature and each spectrum was collected for approximately 300 s at each pressure point. For each spectrum, five data sets were collected and combined to ensure the consistency of the data.

3. Results and Discussion

3.1 Pressure-Induced Modifications in the Raman Spectra

Selected Raman spectra of single-crystal PETN on isothermal compression at room temperature to 26.2 GPa are presented in figure 2. The frequencies of the vibrational bands are plotted as a function of pressure in figure 3. At ambient conditions, PETN belongs to the S_4 point group and has 81 internal lattice vibrations distributed among three symmetry representations (Γ_g = 20A + 21B + 20E) of which, all are Raman active. The fundamental vibrations of PETN are well known at room temperature above 400 cm^{-1}, and detailed normal mode analyses are not reexamined here (*14*, *23*).

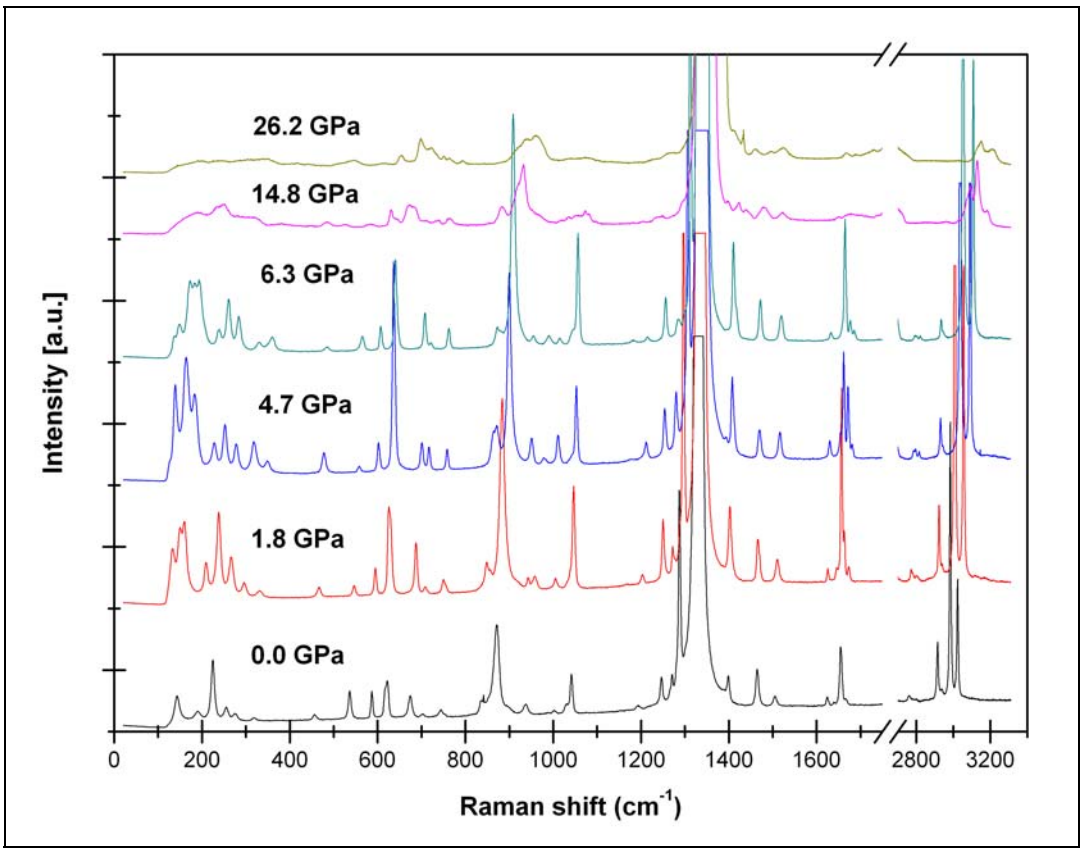

Figure 2. Typical Raman spectra of single-crystal PETN with a neon pressure medium. (The Raman profiles are vertically scaled for the sake of clarity. The spectral range between 1200 cm^{-1} and 1400 cm^{-1} is dominated by the strong first order scattering from the diamond anvils. The spectral region between 1700 cm^{-1} and 3000 cm^{-1} is omitted because of the low vibrational intensity observed within this range.)

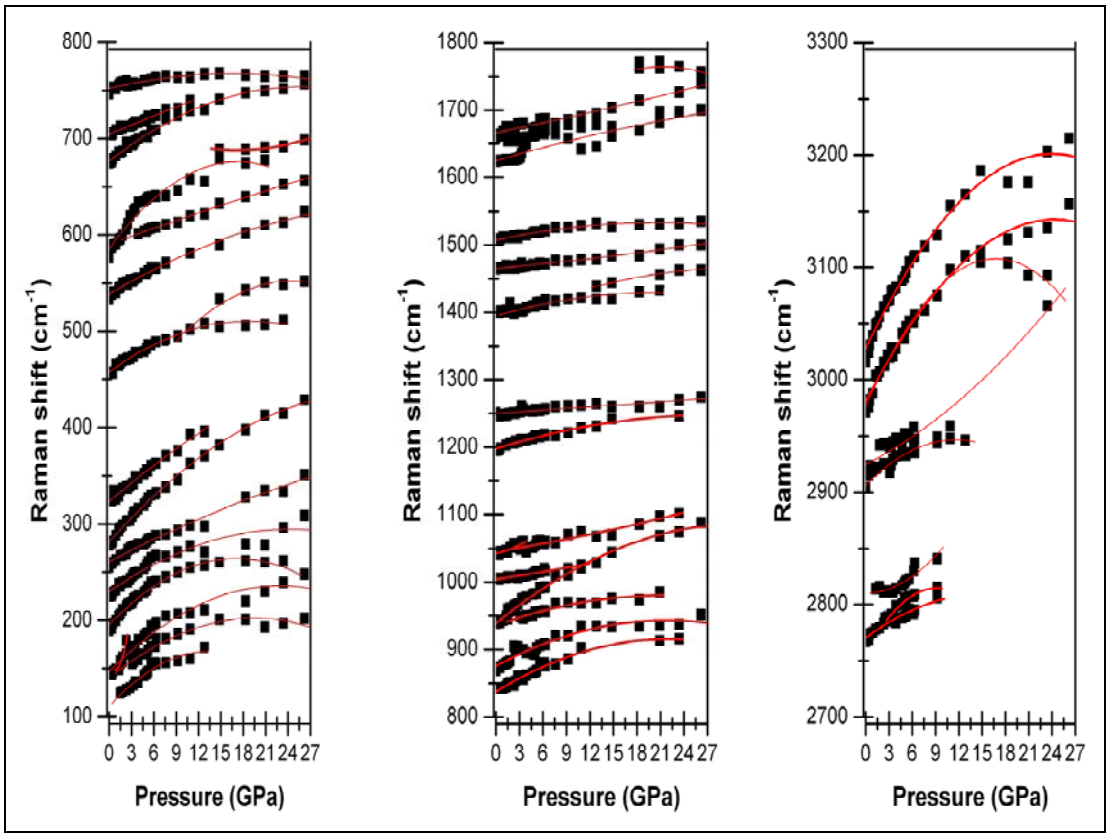

Figure 3. Pressure-driven frequency shifts of PETN Raman scattering peaks between ambient pressure and 26.2 GPa. (The positions of all peaks gradually shift with increasing pressure toward higher energies. Lines are drawn to guide the eye.)

Unusual cracking was observed in the PETN crystal, beginning at pressures near 14.8 GPa, which coincides with a generalized pressure-induced broadening of the Raman vibrational features, as well as the disappearance of several vibrational features. Pressure-dependent broadening of the spectral lines typically results from large modifications in the molecular interactions, and the degree of broadening strongly depends on the density packing of the molecule. This behavior is well documented in PETN, which has been shown to display anisotropic elastic-plastic deformation because of the activation of different slip planes when PETN is subjected to dynamic pressure along different orientations (*4–6*, *8*). Under dynamic compression between 5 GPa and 15 GPa, activation of these slip planes resulted in ionic reactions that led to decomposition of the material (*24*). When the pressure was slowly released from above 14.8 GPa, the cracks rapidly propagated throughout the crystal. There was a slight recovery of the spectral intensity, and several vibrational features reappeared near 3 GPa, possibly because of elastic relaxation. However, upon return to ambient pressure, the crystal abruptly decomposed into a black unknown phase with a featureless Raman spectrum. Similar decompositions are observed in other energetic materials, such as Octahydro-1, 3, 5, 7-tetranitro-1, 3, 5, 7-tetrazocine (HMX) and RDX, and this phenomenon is most likely caused by structural

destabilization that occurs because of the large modifications in the intermolecular interactions and distortions.

3.1.1 Frequency Range 2800–3200 cm^{-1}

The pressure-induced changes in the CH-stretching modes are shown in figures 2 and 3. At ambient conditions, three clearly resolvable modes appear in the spectra at 2904 cm^{-1}, 2971 cm^{-1}, and 3016 cm^{-1}. A small shoulder is noted near 2915 cm^{-1} as well as another CH_2 stretching mode near 2765 cm^{-1}. Figure 3 shows that all modes shift toward higher frequencies with an average rate of (dv/dP) 5.5 cm^{-1}/GPa. On average, the CH-stretching modes show larger pressure dependence than the other internal modes.

Several modifications are immediately noticeable in this spectral region as a function of pressure. The vibrational mode at 2767 cm^{-1} first splits into a doublet near 1.8 GPa, and then another split occurs at 3.3 GPa. The intensities and resolution of these modes diminish abruptly near 14.8 GPa. The symmetric CH-stretching mode near 2900 cm^{-1} splits into a doublet around 14.8 GPa. Because of the shifting of the frequencies with pressure, the 2915 cm^{-1} shoulder becomes a well-resolved maximum above 6.3 GPa. Near 14.8 GPa, all vibrational modes in this spectral region begin to collapse into a single broad peak, but four vibrational maxima can still be discerned. The quartet of peaks collapses to a doublet between 14.8 GPa and 26.2 GPa.

Although the spectra obtained in this energy range display large frequency shifts as a function of pressure, the lack of abrupt discontinuities in the frequency shifts, as evidenced from figure 3, suggests that these modifications arise from a symmetry change. Commonly, abrupt frequency shifts of 50 cm^{-1} or larger, as well as the appearance/disappearance of peaks and in some cases splitting of vibrational modes, characterize high-pressure phase transitions. Similarly, the splitting of vibrational modes and the appearance/disappearance of vibrational peaks also suggest symmetry modifications, but typically, a nearly linear increase in frequency is observed. A comparison of the calculated vibrational spectra for several different conformers to the experimental high-pressure spectra of PETN reveals similarities between the spectra for the D_2 molecular geometry. This molecular symmetry contrasts the study by Gruzdkov et al., which indicated a C_2 molecular symmetry above 5 GPa (*14*). However, the "floppy" molecular structure of PETN is extremely sensitive to pressure gradients that exist in the medium, and differences in the high-pressure molecular symmetry between this study and the Gruzdkov et al. (*14*) study could arise from these pressure gradients within the diamond anvil cell.

3.1.2 Frequency Range 1200–1700 cm^{-1}

The pressure effect on the Raman spectra in this frequency range is shown in figures 2 and 3. Within this energy range, only small modifications in the spectral signature are observed as a function of pressure.

There is a slight intensity increase of the 1261 cm^{-1} C-H bending mode between ambient pressure and 4.7 GPa. Above 4.7 GPa, the intensity gradually diminishes with increasing

pressure. The mode becomes a broad shoulder on the 1200–1350-cm^{-1} first order diamond vibron near 14.8 GPa and at higher pressures, is masked by the diamond vibron. The intensity fluctuations in this vibrational mode likely result from small modifications in the Raman cross section because of modifications of the interlayer coupling and intermolecular interactions as a function of pressure.

In addition to the two-fold increase in intensity of the NO_2 asymmetric stretch near 1660 cm^{-1} between ambient pressure and 1.8 GPa, a small shoulder appears. At 4.7 GPa, the "parent" vibration at 1660 cm^{-1} decreases slightly in intensity and the shoulder shows a slight intensity increase, likely because of an "intensity borrowing" made possible by a resonance enhancement. As pressures continue to increase, the shoulder shows a generalized decrease in intensity while the intensity of the primary mode remains fairly constant. At 14.8 GPa, many bands in this spectral range disappear, similar to the CH-stretching region. The disappearance and/or sudden decreases in the vibrational intensities can be attributed to abrupt changes in the intermolecular interactions, which may be enhanced by dislocations that occur along the shear plane as the slip planes are activated.

3.1.3 Frequency Range 100–1200 cm^{-1}

Typical Raman spectra at several pressures in the frequency range of 100–1200 cm^{-1} are shown in figure 2, and the effect of pressure on individual frequencies is shown in figure 3. Similar to the other vibrational ranges previously examined, modifications are observed in the spectral patterns as a function of pressure but again are not significant enough to suggest a phase transition. Instead, the changes suggest a modification of the molecular geometry that results in a different molecular symmetry.

The following changes are immediately noticeable in the spectra over the pressure range studied. (1) The 145 cm^{-1} C-C torsional mode splits into a triplet between ambient pressure and 1.8 GPa. At pressures near 6.3 GPa, the mode splits again. (2) The NO_2 scissoring mode near 675 cm^{-1} splits into a doublet near 1.8 GPa, and intensity fluctuations are observed over the pressure range studied, which are consistent with a resonant enhancement of the modes near 4.7 GPa. A shifting of the electronic density as compression and densification occur is likely the cause of the resonance enhancement of this mode. (3) Several other vibrational modes, particularly the NO_2 rock near 460 cm^{-1}, the ONO_2 rock near 600 cm^{-1}, and the O'N stretch near 870 cm^{-1}, show a slight increase of intensity to pressures of 4.7 GPa, thus suggesting that small modifications in the Raman cross section occur as the inter-layer coupling changes because of the modification of the molecular geometry under pressure. There is a generalized decrease in intensity of these vibrational features between 4.7 GPa and 6.3 GPa. Many of the vibrational features within this spectral range disappear or become very broad at and above 14.8 GPa because of the formation of dislocations in the lattice resulting from the cracking of the crystal along the slip planes.

The spectral pattern observed between 500 and 800 cm^{-1} is consistent with the S_4 molecular symmetry at ambient pressure. At pressures higher than 6.0 GPa, comparisons of the experimental spectra with Gruzdkov's simulated Raman spectra of the several conformers of PETN show that similarities exist between the calculated spectrum of the D_2 conformer and the experimental spectra, which corroborates the observations noted in the C-H stretching region (*14*).

3.2 Effect of Pressure Media on the High-Pressure Behavior

It is well known that molecular crystals, including energetic materials, are sensitive to pressure gradients because of their low symmetry and threshold for inelastic deformation. Pressure gradients and non-hydrostatic compression within the diamond anvil cell can result in irreversible crystalline modifications at high pressure because of the formation of structural defects (*25*, *26*) or the initiation of chemical reactions (*27*). As a result, the information derived from such experiments can lead to conflicting evidence concerning the high-pressure behavior. In order to fully investigate PETN during high-pressure conditions, we performed several experiments employing different gases as pressure media, each with varying degrees of hydrostaticity: (a) nitrogen - which remains quasi-hydrostatic to 3 GPa; (b) neon - which remains hydrostatic up to 5 GPa and quasi-hydrostatic to near 20 GPa; (c) helium - which remains quasi-hydrostatic to pressures above 50 GPa (*28*), and (d) no pressure media in order to simulate non-hydrostatic conditions with primarily uniaxial compression. We also tested the variation of the high-pressure behavior with a polycrystalline sample and a single crystal of PETN using a neon pressure medium.

Figures 4–7 present selected Raman spectra of PETN, compressed with the various pressure media discussed previously, at the selected pressures of 1.1 GPa, 4.5 GPa, 6.2 GPa, and 9.5 GPa. Although most of the vibrational peaks fall in the same position in all media, several modifications are primarily intensity variations that warrant further discussion.

At 1.1 GPa, the intensity of the 125-cm^{-1} C-C-O wag is much larger in the single-crystal (SC) non-hydrostatic sample than in the other media. Although not as strong as that observed in the non-hydrostatic spectrum, the intensity of this mode is also quite large in the powder sample. From these observations, it is easy to suggest that the prominence of this vibrational feature may be attributable to strain in the molecule, which results in a generalized shift of electronic density and a corresponding modification of the Raman cross section. Because of the "floppy" molecular geometry of PETN, the C-C-O linkages deform quite easily from the ambient S_4 molecular symmetry. It is also interesting to note the fluctuation of the intensity of this C-C-O peak in the SC-neon sample as the pressure is increased. First, it abruptly increases near 4.5 GPa and then decreases at higher pressures. Although the exact of cause of the intensity variation is unclear, it could partially result from the freezing of the neon near 4.5 GPa (*29*).

The intensity of the mode at 278 cm^{-1} (1.1 GPa) also varies strongly with pressure media, with the most intense feature observed in the SC-neon spectrum. Although both features are not resolvable, this vibrational maximum arises from two combination bands: (a) the 23-cm^{-1} O-NO_2 twisting motions about the C-O bonds combined with the 255-cm^{-1} O-NO_2 rocking motions, and (b) the 53-cm^{-1} O-NO_2 twisting motion about the C-O bonds combined with the 225-cm^{-1} C-O-NO_2 rock (*30*). A thorough comparison of figures 4–7 shows that the intensity variation of this feature is not pressure dependent but is only influenced by the pressure media. As previously discussed, the C-O bonds are very sensitive to distortion, but because the fundamental vibrational modes were not observed in our study, it is difficult to offer suggestions for the cause of the variations in intensity between the samples.

The intensity of the 577-cm^{-1} C-C bend and O-NO_2 rock also varies with pressure media. This vibrational maximum is most intense in the powder sample at 1.1 GPa, although it is a resolvable feature in all the single-crystal samples except in the sample with the nitrogen media. This vibrational feature does not appear in the spectrum of the SC-nitrogen sample and disappears

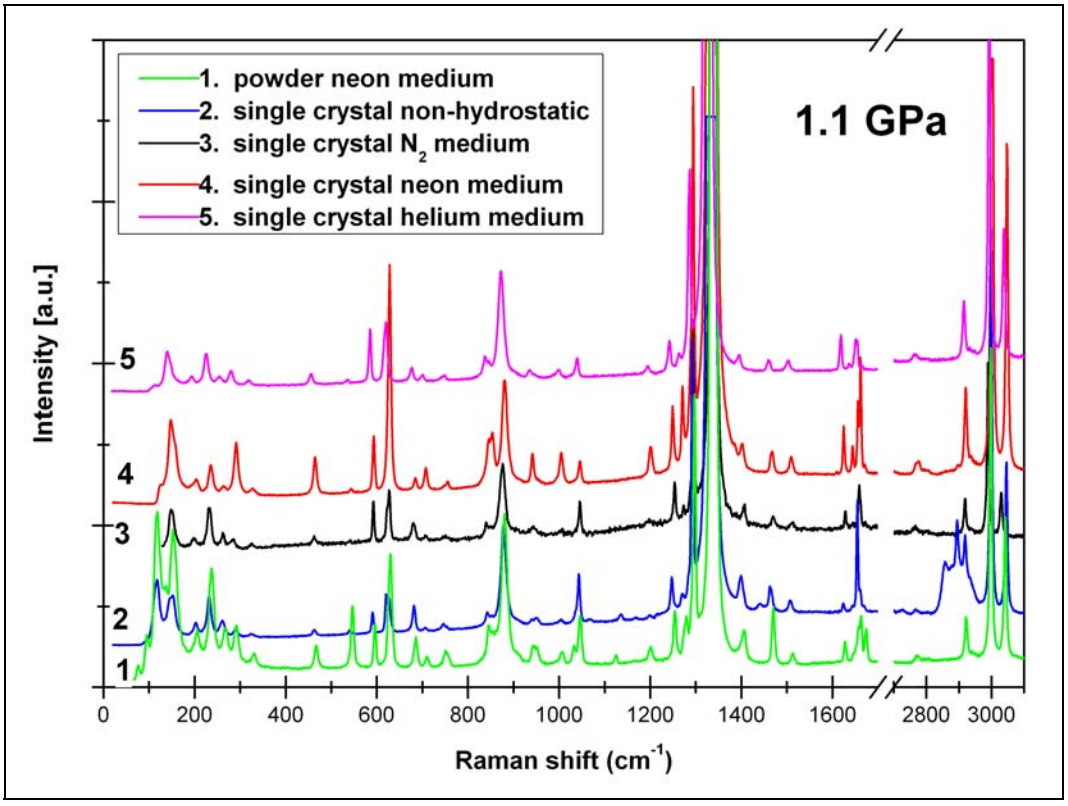

Figure 4. Comparisons of the PETN Raman spectra obtained with different pressure media and crystalline forms at 1.1 GPa. The spectra are scaled vertically for clarity. (The spectral region from ~1250 cm^{-1} to 1375 cm^{-1} is dominated by the strong first order scattering from the diamond anvils. The region from 1750 cm^{-1} to 2700 cm^{-1} is omitted because of the low vibrational intensity and the broad second order diamond vibration within this range.)

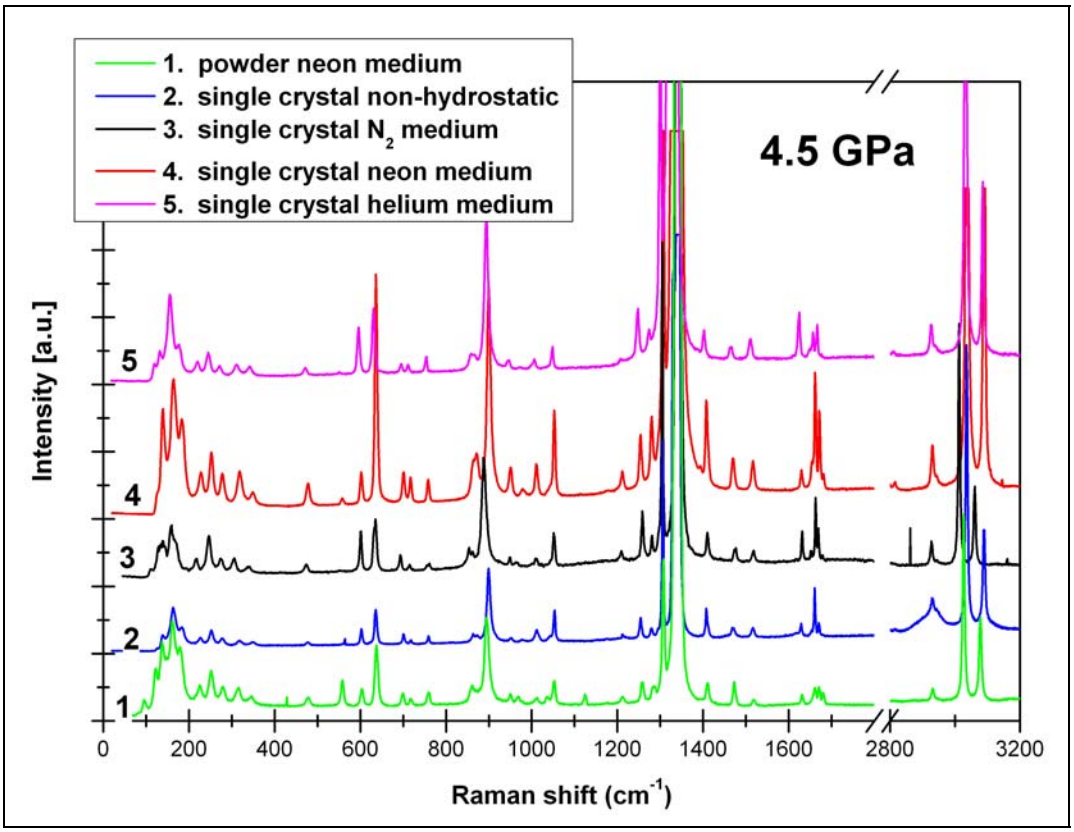

Figure 5. Comparisons of the PETN Raman spectra obtained with different pressure media and crystalline forms at 4.5 GPa. The spectra are scaled vertically for clarity. (The spectral region from ~1250 cm^{-1} to 1375 cm^{-1} is dominated by the strong first order scattering from the diamond anvils. The region from 1750 cm^{-1} to 2700 cm^{-1} is omitted because of to the low vibrational intensity and the broad second order diamond vibration within this range.)

from the spectra of the SC-non-hydrostatic and the SC-helium samples by 6.2 GPa. It is somewhat surprising to note that near 6.2 GPa, the intensity of the mode is similar in both the powder-neon and the SC-neon samples, which indicates that the effects from the grain boundaries may not be a large factor in the stress state of the sample at these low pressures. However, at 9.5 GPa, the vibration becomes more intense in the powder sample than the neighboring O-N stretch, while in the SC-neon sample, the intensity remains fairly constant.

A thorough comparison of figures 4–7 shows that the intensity variation of pattern of the 704-cm^{-1} mode, which has contributions from O-NO_2 stretching, C-C stretching, and NO_2 scissoring, and the 750-cm^{-1} mode, with contributions from the C-C-C deformation and the O-N stretch, varies with pressure medium. At 1.1 GPa, the lower energy 704 cm^{-1} is more intense than the higher energy 750 cm^{-1} vibration in all but the SC-neon sample. Figure 5 shows that the two vibrational modes become nearly equal in intensity in the SC-neon and helium samples by 4.5 GPa. At 6.2 GPa, the intensity pattern is reversed in the SC-neon sample and the O-NO_2

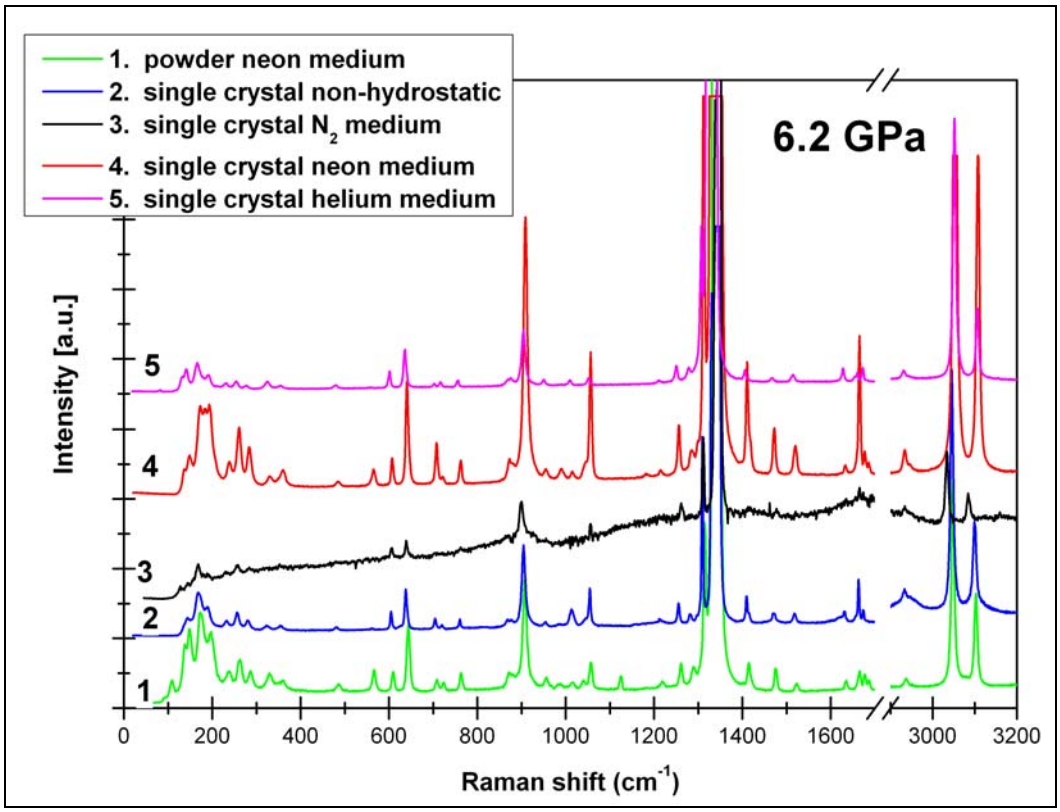

Figure 6. Comparisons of the PETN Raman spectra obtained with different pressure media and crystalline forms at 6.2 GPa. The spectra are scaled vertically for clarity. (The spectral region from ~1250 cm^{-1} to 1375 cm^{-1} is dominated by the strong first order scattering from the diamond anvils. The region from 1750 cm^{-1} to 2700 cm^{-1} is omitted because of the low vibrational intensity and the broad second order diamond vibration within this range.)

stretching, C-C stretching, and NO_2 scissoring, mode is more intense than the C-C-C deformation and the O-N stretching mode. The intensity reversal likely results from a resonance enhancement of the modes, caused by the changes in the molecular symmetry as well as the local environmental effects resulting from the pressure medium.

At 1.1 GPa, there are substantial intensity variations in the vibrational modes between 900 and 1100 cm^{-1}. In the powder and SC-nonhydrostatic samples, the 940-cm^{-1} CH_2 torsional mode appears to be a weak doublet, while only a single vibrational mode is observed in the other single-crystal samples. The splitting likely results from factor group splitting caused by the pressure gradients that exist within the diamond anvil cell. By 4.5 GPa, a weak splitting is also observed in the SC-nitrogen sample, but the doublet collapses into a singlet by 6.3 GPa, probably because of the symmetry change.

The vibrational pattern of the NO_2 stretching modes between 1600 cm^{-1} and 1700 cm^{-1} varies strongly with pressure media. In the powder-neon sample, three maxima are resolvable at 1628 cm^{-1}, 1661 cm^{-1}, and 1672 cm^{-1} with a small shoulder at 1652 cm^{-1}. In the SC-non-hydrostatic, SC-nitrogen, and SC-helium samples, only three peaks are discernible. Similar to the powder-

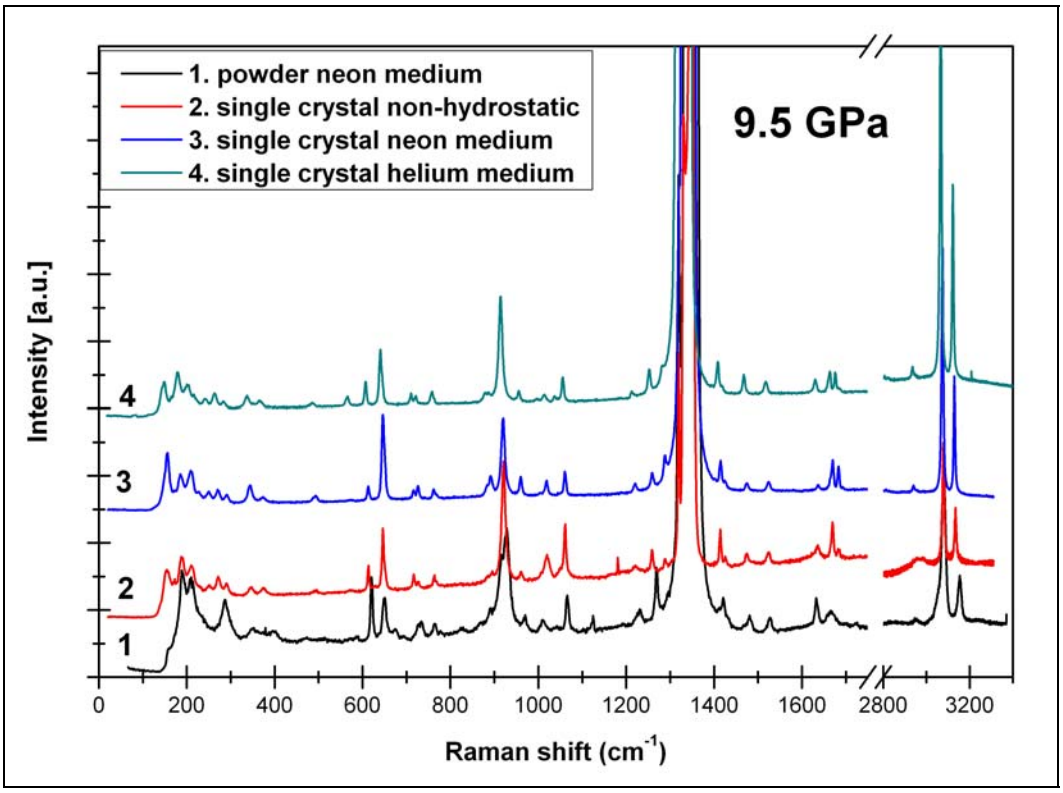

Figure 7. Comparisons of the PETN Raman spectra obtained with different pressure media and crystalline forms at 9.5 GPa. The spectra are scaled vertically for clarity. (The spectral region from ~1250 cm^{-1} to 1375 cm^{-1} is dominated by the strong first order scattering from the diamond anvils. The region from 1750 cm^{-1} to 2700 cm^{-1} is omitted because of the low vibrational intensity and the broad second order diamond vibration within this range.)

neon sample, four peaks are resolvable in the SC-neon sample, but the shoulder is better resolved in the single-crystal sample than in the powder sample. As the pressure is increased to 4.5 GPa, all samples show four resolvable vibrational maxima. By 6.2 GPa, however, the features begin to collapse and there is a generalized weakening of the spectral intensity. As previously discussed, these small variations in the spectral profile are more than likely attributable to symmetry modifications that occur in the molecule as pressure is increased.

There is a large variation in the vibrational pattern of the C-H stretching modes, particularly for the SC-non-hydrostatic sample. A rather broad band is observed near 2900 cm^{-1} with three resolvable maxima. This triplet of bands may be coincidental with factor group splitting of the C-H vibrational stretching mode from the strong uniaxial compression. At higher pressures, the triplet collapses into a broad singlet. At 1.1 GPa, there is also an occurrence of factor group splitting in the SC-nitrogen sample for the C-H stretching mode near 3015 cm^{-1}. By 4.5 GPa, however, the doublet has collapsed back into a singlet.

With the modifications observed in the vibrational spectra as a function of pressure media, justification for the conflicting reports on the high-pressure behavior of PETN becomes apparent.

This study provides strong evidence for a symmetry modification at higher pressures rather than a phase transition, but the transition pressure of the symmetry modification is largely associated with the onset of non-hydrostatic conditions within the diamond anvil cell. The critical pressure occurs between 1.1 GPa and 4.5 GPa in the SC-nitrogen sample. In the case of the powder-neon sample, the onset pressure is between 6.2 and 9.5 GPa, which is somewhat surprising, considering that neon has been shown to remain quasihydrostatic to near 20 GPa. However, interactions at the grain boundaries may play a role in the behavior of this sample during these conditions. Within the pressure range studied, the SC-neon and SC-helium showed similar vibrational behavior because both media remain quasihydrostatic above 10 GPa. At pressures of 14.8 GPa and beyond, both samples underwent the elastic deformation and were not recoverable upon pressure release. These results indicate that hydrostaticity within diamond anvil cells is an important parameter for high-pressure investigations of energetic materials.

4. Conclusions and Summary

Modifications in the Raman spectral signatures of PETN single crystals with a neon pressure medium were examined as high as 26.2 GPa. It is proposed that the main effect of pressure on the PETN structure below 14.8 GPa is a molecular symmetry modification from S_4 to D_2. A number of abrupt changes in the spectra above 14.8 GPa, including peak broadening and the disappearance of several vibrational features, strongly indicate the onset of an elastic-plastic deformation, which occurs from activation of the slip planes. Pressure release indicates that the elastic deformation is somewhat reversible to near 3 GPa, but in all trials conducted with single-crystal samples, the material decomposed upon return to ambient conditions. This behavior of PETN has been observed in shock wave experiments, but it is the first report of it within the diamond anvil cell. All previous diamond anvil cell experiments stopped near 10 GPa (*13*, *14*) or used powered samples (*15*, *16*, *19*). Although this work provides strong evidence for the symmetry transition near 6.2 GPa and the elastic-plastic deformation at 14.8 GPa, ultimately, x-ray diffraction measurements are required to determine the exact behavior.

The high-pressure behavior of PETN was also studied with the use of several pressure media with varying degrees of hydrostaticity. Although the transition pressure of the symmetry modification was found to be largely associated with the onset of non-hydrostatic conditions within the diamond anvil cell, the onset of the elastic-plastic deformation in the single-crystal samples remained constant. These results indicate that hydrostaticity within diamond anvil cells is an important parameter for high-pressure investigations of energetic materials.

5. References

1. Cady, H. H.; Smith, L. C. Studies on the Polymorphs of HMX. Los Alamos Technical Report No. LAMS-2652, 1962.

2. Halleck, P. M.; Wackerle, J. Dynamic Elastic-Plastic Properties of Single-Crystal Pentaerythritol Tetranitrate. *J. Appl. Phys.* **1976**, *47*, 976.

3. Olinger, B.; Halleck, P. M.; Cady, H. H. The Isothermal Linear and Volume Compression of Pentaerythritol Tetranitrate (PETN) to 10 GPa (100 kbar) and the Calculated Shock Compression. *J. Chem. Phys.* **1975**, *62*, 4480.

4. Dick, J. J. Effect of Crystal Orientation on Shock Initiation Sensitivity of Pentaerythritol Tetranitrate Explosive. *Appl. Phys. Lett*. **1984**, *44*, 859.

5. Dick, J. J.; Mulford, R. N.; Spencer, W. J.; Pettit, D. R.; Garcia, E.; Shaw, D. C. Shock Response of Pentaerythritol Tetranitrate Single Crystals. *J. Appl. Phys.* **1991**, *70*, 3572.

6. Dick, J. J. Single Crystal Orientation Effects in Shock Initiation of PETN Explosive. *Los Alamos Technical Report, LA-UR-91-3413*, 1991.

7. Dick, J. J.; Ritchie, J. P. Molecular Mechanics Modeling of Shear and the Crystal Orientation Dependence of the Elastic Precursor Shock Strength in Pentaerythritol Tetranitrate. *J. Appl. Phys.* **1994**, *76*, 2726.

8. Dick, J. J., Anomalous Shock Initiation of Detonation in Pentaerythritol Tetranitrate Crystals. *J. Appl. Phys.* **1997,** *81*, 601.

9. Dick, J. J.; von Dreele, R. B. Determination of the Response of Pentaerythritol Tetranitrate to Static High Pressure up to 4.28 GPa by Neutron Diffraction. *AIP Conf. Proc.* **1998**, *429*, 827.

10. Sorescu, D. C.; Rice, B. M.; Thompson, D. L. Theoretical Studies of the Hydrostatic Compression of RDX, HMX, HNIW, and PETN Crystals. *J. Phys. Chem. B* **1999**, *103*, 6783.

11. Yoo, C. S.; Holmes, N. C.; Souers, P. C.; Wu, C. J.; Ree, F. H.; Dick, J. J. Anisotropic Shock Sensitivity and Detonation Temperature of Pentaerythritol Tetranitrate Single Crystal. *J Appl. Phys.* **2000**, *88*, 70.

12. Dreger, Z. A.; Gruzdkov, Y. A.; Gupta, Y. M.; Dick, J. J. Shock Wave Induced Decomposition Chemistry of Pentaerythritol Tetranitrate Crystals: Time-Resolved Emission Spectroscopy. *J. Phys. Chem. B* **2002**, *106*, 247.

13. Park, T.-R.; Dreger, Z. A.; Gupta, Y. M. Raman Spectroscopy of Pentaerythritol Single Crystals under High Pressures. *J. Phys. Chem. B* **2004**, *108*, 3174.

14. Gruzdkov, Y. A.; Dreger, Z. A.; Gupta, Y. M. Experimental and Theoretical Study of Pentaerythritol Tetranitrate Conformers. *J. Phys. Chem. A* **2004,** *108*, 6216.

15. Lipinska-Kalita, K. E.; Pravica, M. G.; Nicol, M. Raman Scattering Studies of the High-Pressure Stability of Pentaerythritol Tetranitrate, $C(CH_2ONO_2)_4$. *J. Phys. Chem. B* **2005**, *109*, 19223.

16. Ciezak, J. A.; Byrd, E. F. C.; Rice, B. M. Exploring the High-Pressure Behavior of PETN: A Combined Quantum Mechanical and Experimental Study. *Proceedings of the 25th Army Science Conference*, **2006**, in press.

17. Hemmi, N.; Dreger, Z. A.; Gruzdkov, Y. A.; Winey, J. M.; Gupta, Y. M. Raman Spectra of Shock Compressed Pentaerythritol Tetranitrate Single Crystals: Anisotropic Response. *J. Phys. Chem. B* **2006**, *110*, 20948.

18. Green, L. G.; Lee, E. L. Detonation Pressure Measurements on PETN. *Proceedings of Int. Det. Symposium*, **2006**, in press.

19. Lipinska-Kalita, K. E.; Pravica, M. G.; Nicol, M. High-Pressure Synchrotron Radiation X-Ray Diffraction Studies of Pentaerythritol Tetranitrate $C(CH_2ONO_2)_4$, In prepartation.

20. Mao, H. K.; Xu, J.; Bell, P. M. Calibration of the Ruby Pressure Gauge to 800kbar Under Quasihydrostatic Conditions. *J. Geophys. Res.* **1986**, *91*, 4673.

21. Jayaraman, A. Diamond Anvil Cell and High-Pressure Physical Investigations. *Rev. Mod. Phys.* **1983**, *55*, 65.

22. Adar, F. Evolution and Revolution of Raman Instrumentation – Application of Available Technologies to Spectroscopy and Microscopy in *Handbook of Raman Spectroscopy: From the Research Laboratory to the Process Line*, I.R. Lewis and H.G.M. Edwards; Eds. Marcel Dekker, Inc.: New York, NY, **2001**, 11–41.

23. Gruzdkov, Y. A.; Gupta, Y. M. Vibrational Properties and Structure of Pentaerythritol Tetranitrate. *J. Phys. Chem. A* **2001**, *105*, 6197.

24. Gruzdkov, Y. A.; Gupta, Y. M. Experimental and Theoretical Study of Pentaerythritol Tetranitrate Conformers, *J. Phys. Chem. A* **2000**, *104*, 11169.

25. Dreger, Z. A.; Lucas, H.; Gupta, Y. M. High-Pressure-Induced Phase Transitions in Pentaerythritol: X-Ray and Raman Studies. *J. Phys. Chem. B* **2003**, *107*, 9268.

26. Dreger, Z. A.; Gupta, Y. M. High Pressure Raman Spectroscopy of Single Crystals of Hexahydro-1,3,5-trinitro-1,3,5-triazine (RDX). *J. Phys. Chem. B* **2007**, in press.

27. Yoo, C. S.; Cynn, H. Equation of State, Phase Transition, Decomposition of β-HMX (Octahydro-1,3,5,7-Tetranitro-1,3,5,7-Tetrazocine) at High Pressures. *J. Chem. Phys.* **1999**, *111*, 10229.

28. Angel, R. J.; Bujak, M.; Zhao, J.; Gatta, G. D.; Jacobsen, S. D. Effective Hydrostatic Limits of Pressure Media for High-Pressure Crystallographic Studies. *J. Appl. Cryst.* **2007**, *40*, 26.

29. Hemley, R. J.; Zha, C. S.; Jephcoat, A. P.; Mao, H. K.; Finger, L. W.; Cox, D. E. X-Ray Diffraction and Equation of State of Solid Neon to 110 GPa. *Phys. Rev. B* **1989**, *39*, 11820.

30. Allis, D. G.; Korter, T. M. Theoretical Analysis of the Terahertz Spectrum of the High Explosive PETN. *ChemPhysChem* **2006**, *7*, 2398

NO. OF
COPIES ORGANIZATION

1 (PDF ONLY) DEFENSE TECHNICAL INFORMATION CTR
DTIC OCA
8725 JOHN J KINGMAN RD
STE 0944
FORT BELVOIR VA 22060-6218

1 US ARMY RSRCH DEV & ENGRG CMD
SYSTEMS OF SYSTEMS INTEGRATION
AMSRD SS T
6000 6TH ST STE 100
FORT BELVOIR VA 22060-5608

1 DIRECTOR
US ARMY RESEARCH LAB
IMNE ALC IMS
2800 POWDER MILL RD
ADELPHI MD 20783-1197

3 DIRECTOR
US ARMY RESEARCH LAB
AMSRD ARL CI OK TL
2800 POWDER MILL RD
ADELPHI MD 20783-1197

ABERDEEN PROVING GROUND

1 DIR USARL
AMSRD ARL CI OK TP (BLDG 4600)

NO. OF COPIES ORGANIZATION

1 DIRECTOR
US ARMY RSRCH LAB
AMSRD ARL D
J MILLER
2800 POWDER MILL RD
ADELPHI MD 20783-1197

2 COMMANDER
US ARMY RSRCH OFC
TECH LIB
D MANN
PO BOX 12211
RESEARCH TRIANGLE PARK NC
27709-2211

2 DIRECTOR
US ARMY RSRCH LAB
AMSRD ARL RO P
R SHAW
TECH LIB
PO BOX 12211
RESEARCH TRIANGLE PARK NC
27709-2211

4 COMMANDER
NAVAL RSRCH LAB
TECH LIB
CODE 4410
K KAILASANATE
J BORIS
E ORAN
WASHINGTON DC 20375-5000

1 OFFICE OF NAVAL RSRCH
CODE 473
J GOLDWASSER
800 N QUINCY ST
ARLINGTON VA 22217-9999

2 COMMANDER
NSWC
S MITCHELL
C GOTZMER
TECH LIB
INDIAN HEAD MD 20640-5000

1 COMMANDER
NSWC
R HUBBARD
DAHLGREN VA 22448-5000

NO. OF COPIES ORGANIZATION

1 COMMANDER
NAWC
INFO SCI DIV
CHINA LAKE CA 93555-6001

2 COMMANDER
NAWC
CODE 3895
CH1NA LAKE CA 93555-6001

1 WL MNME
ENERGETIC MTRL BR
2306 PERIMETER RD
STE 9
EGLIN AFB FL 32542-5910

1 DIRECTOR
SANDIA NATL LAB
M BAER
DEPT 1512
PO BOX 5800
ALBUQUERQUE NM 87185

2 DIRECTOR
LLNL
ALFRED BUCHINGHAM L 023
MILTON FINGER L 020
PO BOX 808
LIVERMORE CA 94550-0622

1 CIA
J BACKOFEN
RM 4PO7 NHB
WASHINGTON DC 20505

2 SRI INTRNTL
TECH LIB
PROPULSION SCI DIV
333 RAVENWOOD AVE
MENLO PARK CA 94025-3493

1 CDR US ARMY ARDEC
TECH LIB
BLDG 59
PICATINNY ARSENAL NJ
07806-5000

1 AIR FORCE RSRCH LAB
MNME EN MAT BR
B WILSON
2306 PERIMETER RD
EGLIN AFB FL 32542-5910

NO. OF
COPIES ORGANIZATION

1 AIR FORCE OFC OF SCI RSRCH
M BERMAN
875 N RANDOLPH ST
STE 235 RM 3112
ARLINGTON VA 22203-1768

2 SANDIA NATL LABS
TECH LIB
NM BUILDING 804, MS-0899
ALBUQUERQUE NM 87185

2 LLNL
TECH LIB
PO BOX 808-L610
LIVERMORE CA 94550-0622

2 LOS ALAMOS NATL AB
TECH LIB
MS-P362
PO BOX1663
LOS ALAMOS NM
87545-1362

1 NIST CENTER
FOR NEUTRON RESEARCH
S TREVINO
100 BUREAU DR MS 8562
GAITHERSBURG MD 20899

3 NIST CENTER
FOR NEUTRON RESEARCH
T JENKINS
100 BUREAU DR MS8562
GAITHERSBURG MD 20899

ABERDEEN PROVING GROUND

17 DIR USARL
AMSRD ARL WM
T ROSENBERGER
AMSRD ARL WM M
S MCKNIGHT
AMSRD ARL WM T
B BURNS
AMSRD ARL WM TB
P BAKER
AMSRD ARL WM BD
R BEYER
E BYRD
B FORCH

NO. OF
COPIES ORGANIZATION

J CIEZAK (3 CPS)
K MCNESBY
M MCQUAID
R PESCE-RODRIGUEZ
B RICE
M ZOLTOSKI
AMSRD ARL WM TD
D DANDEKAR